$NdBaMn_2O_{5+\delta}$ Layered perovskite as an active cathode material for solid oxide fuel cells

Abdalla M. Abdalla[1,2,3*],Shahzad Hossain[1,3,4], Jun Zhou[5], Pg M.I.Petra[1],Stene Erikson[6,] Cristian D. Savaniu[3], John T. S. Irvine[3*], Abul K. Azad[1*]

[1]*Faculty of Integrated Technologies, Universiti Brunei Darussalam, Jalan Tungku Link, Gadong BE 1410, Brunei Darussalam*

[2]*Mechanical Engineering Department, Faculty of Engineering, Suez Canal University, Ismailia 41522, Egypt*

[3]*Center for Advanced Material, School of Chemistry, University of St Andrews, Fife KY169ST, UK*

[4]*Institute of Nuclear Science and Technology, Bangladesh Atomic Energy Commission, GPO Box No. 3787, Dhaka 1000, Bangladesh*

[5]*Center of Nanomaterials for Renewable Energy, State Key Laboratory of ElectricalInsulation and Power Equipment, Xi'an Jiaotong University, Xi'an 710049, China*

[6]*Department of Chemistry and Chemical Engineering, Chalmers University of Technology,SE 41296, Sweden*

**Correspondence to:* abdalla.m.a1984@gmail.com/ abul.azad@ubd.edu.bn / jtsi@st-andrews.ac.uk

Abstract

A layered perovskite,$NdBaMn_2O_{5+\delta}$(NBMO), was synthesized by the solid state reaction method in air. Rietveld analysis of X-Ray Diffraction (XRD) data showed the material crystallizing in orthorhombic symmetry (*Pmmm* space group). Scanning electron microscopy (SEM)was used to examine the morphology and, the analysis of the micrographs showed the formation of a porous structure exhibiting in-situ growth of nanoparticles. Electrochemical Impedance Spectroscopy (EIS) measurements from 600°C to 800°Cshows the highest conductivity value of 1.17×10^{-1}S/cm obtained at 800°C with low activation energy (E_a) of 0.3 eV in air. In 5% H_2/Ar gas mixture, the conductivity and activation energy values were 1.97×10^{-2}S/cm and 0.4 eV, respectively at 800°C. The DC conductivity measurements also showed that this material is highly conductive in air with a conductivity value of 0.75 S/cm at 850 °C. Dual chamber fuel cell measurements on Ni-YSZ/YSZ/NBMO cell using 5% H_2/Aras fuel (from 700 °C to 800 °C)shows a maximum power density of 0.202 W/cm^2at 800°C. The relatively high conductivity of the material in air and low activation energy makes it a potential candidate as cathode for solid oxide fuel cells.

Keywords: Layered perovskite; SOFC; Cathode materials; Exsolution; Impedance measurements

1. Introduction

Solid Oxide Fuel Cell (SOFC) technology is very efficient and promising energy conversion system for replacing the existing fossil fuel economy in-line with other types of renewable and alternative energies like solar, wind and biomass [1–7]. The development of new materials to use in fuel cell devices contributes to the achievement of high performance through electrochemical

reactions, along with good durability and life time for these electrochemical devices. The electrochemical transport reactions and the proper characterization of the material depend on the structure at various scales, from atomic level to the microstructural level. This has an important synergistic effect on the performance of the material[7].Recently introduced materials such as $ABO_{3-\delta}$ and $A_2B_2O_{5+\delta}$ perovskite material aimed to use in fuel cells offer the advantage of high electrical and ionic conductivities at higher temperatures[8,9].The electrical properties can be further improved by favorable substitution of either A or B sites of the nominal perovskite with acceptoror donor-type cations [10]. Recent research focuses on lanthanide (Ln) -containing oxide materials doped with alkaline elements (Ba, Sr,Ca, etc.) and transition metals (Cr, Mn, Fe, etc.). Hence, their good mixed electronic and ionic conducting behavior were recognized as very promising (LT, IT, HT-SOFCs)for electrode materials[11–13].However, these materials still exhibit slow oxygen transportation kinetics, specifically with intermediate temperatures of 500–800°C.

The oxygen kinetics in perovskite type structures has been reported showing the significant enhancement of layered types than the disordered perovskites [14]. Furthermore, layered type perovskites [9,15- 21] have shown interesting findings with a superior power density values[9,17,20] under different atmospheres for application as electrode material in SOFC. The novelty of using layered materials provide more powerful, efficient, stable and durable devices especially for intermediate temperatures IT-SOFCs. $PrBaMn_2O_{5+\delta}$ [9] was reported as a new A-site layered perovskite that display superior performance as anode material compared to the $PrBaCo_{2-x}Mn_xO_{5+\delta}$ with various fuels [22]. $NdBaCo_{2-x}Mn_xO_{5+\delta}$ [23] with different values of x are reported to have suitable electrical properties, in addition to being thermally stable cathode materials. In a recent study, the material of $NdBaMn_2O_{5+\delta}$ was investigated [24] with regard to its

structure and electrical conductivity. Hence, $Ln^{3+}$and Ba^{2+}cations order in alternating layered perovskites in $LnBaMn_2O_{5+\delta}$ (*Ln* = lanthanide)[9],[23-26]showing the ability to perform as an electrode material for SOFCs as well as oxygen storage applications[25].

Thus, in this work, $NdBaMn_2O_{5-\delta}$layered perovskite material was synthesized (with an interesting findings of nanoparticles exolusion) by a conventional solid state reaction technique then characterized by using X-Ray Diffraction (XRD), scanning electron microscopy (SEM), direct current (d.c) conductivity, electrochemical impedance spectroscopy (EIS) in both dry air and 5% dry H_2/Ar conditions and electrochemical performance (I-V) using a dual chamber fuel cell arrangement.

2. Experimental

The compound $NdBaMn_2O_{5+\delta}$ was obtained by the solid state reaction route. Stoichiometric amounts of the pre-dried precursors:Nd_2O_3, $BaCO_3$ and Mn_2O_3weremixed in ethanol, dried and ball milled for 24 hours. The mixture was dried in the drying oven again and calcined at 800 °C for 8 hours in air. The powder was mixed again in an agate mortar and pestle, pressed into pellets and fired at 1200 °C for 12 hours in air and then initial XRD phase was checked. After re-grounding and mixing, the final sintering was performed at 1400 °C for 12 hours. The heating and cooling rate was5 °C/min. XRD data were collected using a SIEMENS Diffractometer (D5000 Kristalloflex, Cu Kα1, λ = 1.5406Å) in the range of $10^o \leqslant 2\theta \leqslant 80^o$ with a 0.01step size. Scanning Electron Microscope (SEM) images were collected on a pellet surface using a JSM-7610F. The electrical conductivity was measured in air using a Van Der Pauw, four-probe DC setup. The material was pressed into a rectangular bar and sintered at 1400 °C for two hours. Next, four gold wires were attached on the sample surface with gold paste and fired again at 700 °C for one hour with 2 °C/min heating and cooling rate. Afterwards, the sample was collected and fixed on a special

jig and the four probes were attached to the samples before the whole set up was inserted in to the furnace and tested at temperature range from 30 °C to 850 °C in air at4 °C/min heating and cooling rate.

EIS was measured using Solartron1260 Impedance analyzer with Solartron1255 (Schlumberger) frequency response analyzer (0.01 Hz～1 MHz)in dry air and 5% dry H_2/Ar in the temperature range from 600 °C to 800 °C. The samples for symmetrical cells were prepared using a slurry made by mixing $NdBaMn_2O_5$ powder with an organic vehicle containing terpineol and binder(turpentine). The slurry was then applied onto both sides of a YSZ thick electrolyte (2mm, symmetrical cell setup) by screen-printing method, followed by sintering at 1000°C for two hours in air. The thickness of the electrode coated layer was approximately 30 μm and the electrode area (effective area) was 0.125 cm^2.

Current versus voltage measurements were done using SSL scientific test rigs at the temperature 800 °C and 700 °C with open circuit voltage (OCV) of 0.92 V in dual chamber mode. Single cells were prepared by screen printing the slurries of Ni-YSZ (anode material, 50-50 vol/vol) and $NdBaMn_2O_5$(cathode) on a thin YSZ pellet(2 mm thickness, 20 mm diameter, Fuel Cell Materials, USA) and sintered at 1100°C for 2hours. The thickness of the screen printed layer was about30 μm. Platinum (Pt) current collector was painted to the cathode surface and gold (Au) current collector was painted to the anode surface and fired at 750 °C for 1h with a rate of 2 °C/min.

3. Results and Discussion

3.1 Structural analysis

Figure1(a) shows the Rietveld profile of the obtained X-ray powder diffraction pattern for the layered$NdBaMn_2O_{5+\delta}$using Fullprof software[27]. Schematic 3D crystal structure has been shown in the insert and in Figure 1(b). The XRD pattern was indexed by using STOE Win^{XPOW} software

package[28].The atomic positions were obtained with the help of SPUDS software [29].However, various possible structures of *Ln*BaMn$_2$O$_{5+\delta}$ were reported in the literature [9,18,20] and we obtained the main phase of crystal structure in the orthorhombic symmetry in the (P*mmm*) space group. Hence, a very small amount (~ 5%) of hexagonal phase was observed, with the main phase similar to Thibault et al.[23]. The impurity phase was identified as Nd_2O_3, which can be refined in the rhombohedral symmetry in the *R-3c* space group. Rietveld analysis using both phases together converged in a very good χ^2 value (χ^2 =0.99). Structural symmetry, unit cell parameters, space group, cell volumes, atomic positions and R-factors are listed in Tables 1 and 2.

3.2 Microstructural analysis

Figure 2 shows the SEM image of a pellet surface of the layered NdBaMn$_2$O$_5$.The SEM images indicate that this material has a good porosity with a relative density (ρ) of 82.74%.Densities of the material were measured using structural refinement(theoretically) and Archimedes method [30] (experimentally); and was found to be 6.88 g/cm^3 and 5.68 g/cm^3, respectively. For theoretical density calculation the equation (1) [31]was used;

$$\rho = \frac{Z*F_w}{V*N_a} \qquad (1)$$

Where:ρ is the density, Z is the number of atoms in the asymmetric unit in the unit cell, F_w is the formula weight [kg mol^{-1}], V is the unit cell volume of [m^3] and N_a is the Avogadro's number [atoms mol^{-1}].The theoretical density was measured from bulk using mass per volume in Archimedes procedure. The relative density was calculated from dividing theoretical density by bulk density according to the equation 2 [31]:

$$\text{Relative density (\%)} = \frac{\text{Actual density} - \text{pores(\%)}}{\text{Bulk density}} \qquad (2)$$

where: Actual density - pores (%) is representing the experimental value of density got from Archimedes method (measured) and Bulk density is representing the theoretical value got from reitveled analysis (crystallographic).

There are visible elongated grains well connected to each other which is important for SOFC electrode materials as it provides a pathway for conduction. This type of morphology is important to show an excellent stability and reversibility of oxygen storage-related process[26].

Due to sufficient and well-connected porosity, high ionic transportation is also expected, and allowed the gas flow to diffuse through the cell and results in the escape of the exhaust gas from it as well [32,33].Figure 2(b) shows the enlarged view of the SEM image. A careful observation of the enlarged view in Figure 2 (b) shows the growth of nano-particles on the surface of the grains which basically occurred at higher sintering temperature. An area containing well distributed and uniformly grown of nano-particles is shown in Figure 3 and this formation of nanoparticles is most probably resulted from MnO_2 basedon the study of T. Le et al.[34]showing a great enhancement of electrochemical performance. Formation of nanoparticles is well reported in the literature, e.g. recent reports by Neagu et al.[35]on reduced perovskite material with A-site deficiency for fuel electrode applications. Moreover, Zhou et al.[20] in a very recent study have shown the similar phenomenon with layered perovskite $La_{0.8}Sr_{1.2}Fe_{0.9}Co_{0.1}O_{4-\delta}$(LSFCO). The occurrence of this phenomenon is very important for the enhancement of electocatalytic activity [34] and this growth/nucleation of the particles that decorate the native surface allows enhancing the performance in ion transportation for the electrode which is expected for SOFC devices[2-5].

SEM morphology observations of NBMO electrode was also carried out before and after testing the single cell (see Fig 4b, c). As we can see, the layers are adherent and no delamination

happened. Moreover, the both sides of electrode became more porous and the dense electrolyte attached them without any cracks.

3.3 Electrical conductivity

The d.c. conductivity of the rectangular NBMO bar was measured in air. The conductivity value σ was calculated using Uhilr equation [36].

$$\sigma = \frac{d}{R \times t \times L_{av}} \qquad (3)$$

Where d is the spacing between the voltage wires, t is the bar thickness and L_{av} is the effective length of the bar.

Figure 5 shows the calculated value of the NBMO which exhibits a higher electrical conductivity value of 0.75 Scm^{-1}at 850 °C in air. This conductivity value is influenced by the existence of mixed oxidation states ($Mn^{+4}/Mn^{+3}/Mn^{+2}$ in NBMO)[37].Thus, the change in oxidation state of Mn associated with the presence of Nd^{+3}(based on the structural analysis and from morphological images) that showed the growth of nanoparticles which basically from Mn oxide results in an optimized balanced ratio as a function of electronic charge carrier concentration, leading to this enhancement in the electrical conductivity [38].

3.4 Electrochemical impedance spectroscopy(EIS)

EIS measurements of symmetrical cell $NdBaMn_2O_5|YSZ|NdBaMn_2O_5$ was performed and analyzed by Z-plot software. The data were collected at 600, 650, 700, 750 and 800 °C in air and 5% H_2/Ar. The collected data was fitted with a series of equivalent circuits (see figure 6 insert)in order to obtain the resistance values of the different contributing components to the impedance spectra i.e. bulk, grain, grain boundary, etc. The impedance curves were showing two characteristic semicircles, the dominant one being at low frequency associated with electrode processes[39].The

polarization resistance values in 5% H_2/Ar were much higher than in air (see figure 6 a, b for comparison).

The electrode resistance clearly increases with decreasing temperature. However, the better fitting cannot be obtained without addition of an inductance element, for all the temperature ranges in case of measurements in air.

The actual capacitance can be calculated using the expression given in reference [40]. The capacitance values in this temperature range were 2.76×10^{-3} F to 3.56×10^{-7} F in air and 5.12×10^{-5} F to 4.36×10^{-7}F in 5% H_2/Ar describing processes associated with various electrochemical reactions on the electrode and electrolyte-electrode interface.. The total conductivity of the electrode(σ), the total capacitance (C) and the area specific resistance (ASR) are listed in table 3. The activation energy (E_a)was calculated [41] through the use of the following equations:

$$E_a = -R\left[\frac{\mathrm{d}\ln K(T)}{d(1/T)}\right] \qquad (4)$$

and

$$m = \frac{-E_a}{R} \qquad (5)$$

where; R is the gas constant , T is the temperature, m is the slope of the Arrhenius plot. The significant higher conductivity in air 0.75 Scm^{-1} and low activation energy Ea of 0.3eV at 800 °C compared to H_2-containing atmosphere indicates that these porous electrode are suitable for cathode component; however, a similar material obtained by replacing the Nd by Pr was reported as an anode material [9]. Fig 7 represents the Arrhenius plots of total conductivity measured in air and 5%H_2 in the temperature range of 600 °C– 800 °C.

Figure 8 shows a representation of polarization resistance against temperature for NBMO both in Air and 5% H_2conditions, showing the increase of the polarization resistance with the decrease of temperature[42].However, although in both cases it shows the same trend of increase, in air it still

shows the smaller value of 0.298 Ωcm^2 at 800°C, thus explaining the higher conductivity exhibited in air. This value is also smaller compared to the commonly used cathode materials such as $La_{0.8}Sr_{0.2}MnO_3$(LSM) (4.2Ω cm^2 at 700 °C) [43], and $La_xSr_{1-x}Co_yFe1\text{-}yO_{3-\delta}$(LSCF) (0.34Ω cm^2 at 700 °C) [44].

3.5 Power density measurements

The single cell of Ni-YSZ/YSZ/NBMO was prepared for testing in a dual chamber mode under 5% H_2/Ar fuel from 700 °C to 800 °C with a water bubbling system for humidification (~3% at room temperature). As shown in Fig. 9, the performances were done under open circuit voltage(OCV) with humidified H_2as a function of applied current density. The OCV was 0.92 V for cells with NBMO cathode at 800 °C was found almost in the close range to the theoretical values derived from the Nernst equation where :

$$E_T = E_0 + \frac{RT}{2F} lnpH_2 - \frac{RT}{2F}\ lnpH_2O + \frac{RT}{2F}\ lnp^{\frac{1}{2}}O_2 \qquad (4)$$

which can be noticed from table 4.This value is also very close to the value reported by Kim et al.[10]. No cracks or holes were observed during the testing process of the cells [45], the lower OCV value normallyindicate imperfect sealing. The measurements were done at 800ºC, 750 °Cand 700 °C using air in the cathode side and 5%humidified hydrogen (H_2/Ar) at the anode side (at a flow rate of 100 ml/min). The obtained results are shown in Figure9,representa maximum power density value of 0.202 W/cm^2 at 800ºC which decreases with decreasing temperature. Similar power density was observed by Zhou et al.[20] using $La_{0.8}Sr_{1.2}Fe_{0.9}Co_{0.1}O_{4-\delta}$(LSFC)as a layered perovskite cathode material. A very good performance was obtained by Sengodanet al.[9]using $PrBaMn_2O_5$ PBMO layered anode material with $NdBa_{0.5}Sr_{0.5}Co_{1.5}Fe_{0.5}O_{5+\delta}$-$Ce_{0.9}Gd_{0.1}O_{2-\ \delta}$ NBSCF50-GDC composite cathode material with power density of 1.5 W/cm^2. The good power density in this work is due to the high ionic conductivity associated with electrolyte (support

YSZ)and from the low ASR obtained from the electrodes [46]. This material NBMO is similar to of the materials presented by Adler SB[45].NBMO apparently increase the electrochemical activity of cathode of this cell [45-48].

The non-linearity in I-V measurements for SOFC arises when the amplitude of voltage and current excitation is large. SOFCs are complicated systems containing multiple mass-transfer, chemical and electrochemical processes. The coupling of these processes makes the systems non-linear. The transfer function in a non-linear system reflects the relationship between the voltage and current at different frequencies. The amplitude of the perturbation signal must be small enough to meet the linearity requirement of the transfer function ($Z(j\omega)$). If the amplitude is large, non-linear analysis must be used [49].

Although the power density of our cell is not very high compared to the literature but still it has the potential for the effective use in future after modification and more electrochemical investigations. This low value may be was due to the usage of two different current collectors Pt and Au which results in an increases of the single cell total resistance.

Conclusions

$NdBaMn_2O_5$layered perovskite was synthesized by solid state reaction method in air. Structural characterization of $NdBaMn_2O_5$ was done through XRD and SEM. The electrochemical properties were measured using dc conductivity, impedance and fuel cell tests. The results indicate that this material will be a good candidate as SOFC air electrode. The structural analyses were precisely done for investigating the space group, cell parameters, atomic positions as well as oxygen occupancies. By careful analysis of the peak splitting, we have demonstrated the accurate structural parameters, symmetry and space group (e Orthorhombic, S.G. P*mmm*). SEM images show a porous structure with in-situ growth of nanoparticles which is beneficial to increase

electrochemical performance in the perovskite structure, both single and layered. Meanwhile, dc conductivity measurements indicate that the NBMO is a good electric conductor in air (0.75 Scm^{-1}). The conductivity in air is higher than in 5% H_2/Ar and decreases with decreasing temperature. The power density was found to be 0.202 W/cm^2 at 800 °C, which is reported for the first time in this studies.

4. Acknowledgment

The authors Abdalla. M. Abdalla and Shahzad Hossain are grateful to the GRS unit for funding this researchat Universiti Brunei Darussalam. Authorsare also very grateful to Professor John T. S. Irvine to manage a visiting scholarship for six months for AMA and SH to conduct this work at University of St Andrew's, UK.

References

[1]C. Sun, R. Hui, J. Roller, Cathode materials for solid oxide fuel cells: A review, J. Solis.State Electrochem. 14 (2010) 1125–44.

[2]S. Hossain, A. M. Abdalla, S. N. Binti Jamain, J.H. Zaini, A. K. Azad, A review on proton conducting electrolytes for clean energy and intermediate temperature-solidoxide fuel cells, J. Ren. and Sus.e Ener. Rev.79 (2017) 750–764.

[3] N. Mahato, A. Banerjee, A. Gupta, S. Omar, K. Balani, Progress in material selection for solid oxide fuel cell technology: A review, J. Prog. Mater. Sci. 72 (2015) 141–337.

[4] W.Z. Zhu, S.C. Deevi, A review on the status of anode materials for solid oxide fuel cells, J. Mat. Sci. Eng. A. 362 (2003) 228–239.

[5] Z.P. Shao, W. Zhou, Z.H. Zhu, Advanced synthesis of materials for intermediate-temperature solid oxide fuel cells, J. Prog. Mater. Sci. 57 (2012) 804–874.

[6] Y. Zha, C. XIa, L. Jia, Z. Wang, H. Li, J. Yu, Y. Li, Recent progress on solid oxide fuel cell: Lowering temperature and utilizing non-hydrogen fuels, Int. J. Hydro. Ener. 38 (2013) 16498–16517.

[7] N.H. Menzler, F. Tietz, S. Uhlenbruck, H.P. Buchkremer, D. Stöver, Materials and manufacturing technologies for solid oxide fuel cells, J. Mater Sci, 45 (2010)3109–35.

[8] A.K. Azad, J.H. Kim, J.T.S. Irvine, Structure–property relationship in layered perovskite cathode $LnBa_{0.5}Sr_{0.5}Co_2O_{5+\delta}$ (Ln=Pr, Nd) for solid oxide fuel cells, J. Power Sources. 196 (2011) 7333–7337.

[9] S. Sengodan, S. Choi1, A. Jun, T. Ho Shin, Y. Wan Ju, H. Young Jeong, J. Shin, J. T.S Irvine, G. Kim, Layered oxygen-deficient double perovskite as an efficient and stable anode for direct hydrocarbon solid oxide fuel cells, Nat Mater. 14 (2014) 205–9.

[10] S. Yoo, S. Choi, J. Kim, J. Shin, G. Kim, Investigation of layered perovskite type $NdBa_{1-x}Sr_xCo_2O_{5+1}$ (x = 0, 0.25, 0.5, 0.75 and 1.0) cathodes for intermediate-temperature solid oxide fuel cells, Electrochimica Acta. 100 (2013) 44–50.

[11] H. Rahmouni, B. Cherif, K.Khirouni, M. Baazaoui, S. Zemni, Influence of polarization and iron content on the transport properties of praseodymium–barium manganite, J. Phys Chem Solids. 88 (2016) 35–40.

[12] T. Wen, H. Tu, Z. Xu, O. Yamamoto, A study of (Pr, Nd, Sm)$_{1-x}$Sr$_x$MnO$_3$ cathode materials for solid oxide fuel cell, Solid State Ionics 122 (1999) 25–30.

[13] Y. Wang, H. Zhang, F. Chen, C.Xia, Electrochemical characteristics of nano-structured PrBaCo$_2$O$_{5+x}$ cathodes fabricated with ion impregnation process, J. Power Sources 3 (2012) 34–41.

[14] G. Kim, S. Wang, A. J. Jacobson, L. Reimus, P. Brodersen and C. A. Mims, Rapid oxygen ion diffusion and surface exchange kinetics in PrBaCo$_2$O$_{5+x}$with a perovskite related structure and ordered A cations, J. Mater. Chem. 17 (2007) 2500–2505.

[15] C. Zhu, X. Liu, C. Yi, D. Yan, W. Su, Electrochemical performance of PrBaCo$_2$O$_{5+d}$ layered perovskite as an intermediate-temperature solid oxide fuel cell cathode, J. Power Sources 185 (2008) 193–196.

[16] F. Zhao, S. Wang, K. Brinkman, F. Chen, Layered perovskite PrBa$_{0.5}$Sr$_{0.5}$Co$_2$O$_{5+d}$ as high performance cathode for solid oxide fuel cells using oxide proton conducting electrolyte, J. Power Sources 195 (2010) 5468–5473.

[17] C. Lim, A. Jun, H. J, K. Min Ok, J. Shin, Y. Wan Ju and G. Kim, Influence of Ca-doping in layered perovskite PrBaCo$_2$O$_{5+d}$ on the phase transition and cathodic performance of a solid oxide fuel cell, J. Mater. Chem. A. 4 (2016) 6479- 6486.

[18] S. Choi, S. Sengodan, S. Park, Y.W. Ju, J. Kim, J. Hyodo, H. Y. Jeong, T. Ishihara, J. Shin and G. Kim, A robust symmetrical electrode with layered perovskite structure for direct hydrocarbon solid oxide fuel cells: PrBa$_{0.8}$Ca$_{0.2}$Mn$_2$O$_{5+d}$. J. Mater. Chem. A. 4 (2016)1747-1753.

[19] A. Jun, J. Kim, J. Shin, G. Kim, Optimization of Sr content in layered SmBa$_{1-x}$Sr$_x$Co$_2$O$_{5+d}$ perovskite cathodes for intermediate-temperature solid oxide fuel cells, Int. J. Hydro. Energ. 37 (2012) 18381-18388.

[20] J. Zhou, T.-Ho Shin, C. Ni, G. Chen, K. Wu, Y. Cheng, and J. T. S. Irvine, Insitu Growth of Nanoparticles in Layered Perovskite La$_{0.8}$Sr$_{1.2}$Fe$_{0.9}$Co$_{0.1}$O$_{4-\delta}$ as an Active and Stable Electrode for Symmetrical Solid Oxide Fuel Cells, Chem. Mater., 28, 9 (2016), 2981– 2993.

[22] W. Guo, R. Guo, L. Liu, G. Cai , C. Zhang , C. Wu , Z. Liu, H. Jiang, Thermal and electrochemical properties of layered perovskite PrBaCo$_{2-x}$Mn$_x$O$_{5+d}$ (x= 0.1, 0.2 and 0.3) cathode materials for intermediate temperature solid oxide fuel cells, Int. J. Hydro. Energ. 40 (2015) 12457–12465.

[23] T. Broux, M. Bahout, J. M. Hanlon, O. Hernandez, S.Paofai, A. Berenovb and S. J. Skinner, High temperature structural stability, electrical properties and chemical reactivity of NdBaCo$_{2-x}$MnxO$_{5+\delta}$ ($0 \leq x \leq 2$) for use as cathodes in solid oxide fuel cells, J. Mater. Chem. A. 2 (2014) 17015-17023.

[24] O.L. Pineda,Z.L. Moreno, P. Roussel, K. Świerczek, H.G. Gilles, Synthesis and preliminary study of the double perovskite NdBaMn$_2$O$_{5+\delta}$ as symmetric SOFC electrode material, J Solid State Ionics. 288 (2016) 61–67

[25] F .Tonus, M. Bahout, V. Dorcet, G. H. Gauthier, S. Paofai, R. I. Smith, Stephen T. Skinner, Redox behavior of the SOFC electrode candidate NdBaMn$_2$O$_{5+\delta}$ investigated by high-temperature in situ neutron diffraction: first real-time characterisation of an LnBaMn$_2$O$_{5.5}$ intermediate phase, J. Mater Chem A. 4 (2016) 11635-11647

[26] M. Bahout, S. S. Pramana, J. M. Hanlon, V. Dorcet, R. I. Smith, S. Paofaia and Stephen J. Skinner, Stability of NdBaCo$_{2-x}$Mn$_x$O$_{5+d}$ (x= 0, 0.5) layered perovskites under humid conditions investigated by high-temperature in situ neutron powder diffraction J. Mater. Chem. A. 3 (2015) 15420

[27] J. R.-Carvajal, Recent advances in magnetic structure determination by neutron powder diffraction, Phys B Condens Matter 192 (1993) 55–69.
[28] D. Friedrich, M. Schlosser, A. Pfitzner, Synthesis, Crystal Structure, and Physical Properties of Two Polymorphs of $CsGaSe_2$, and High-Temperature X‑ray Diffraction Study of the Phase Transition Kinetics. J Cryst. Growth Des. 16 (2016) 3983−399.
[29] M.W.Lufaso, P.M.Woodward, Prediction of the crystal structures of perovskites using thesoftware program, J. Acta Crystallography B. (2001) 725–38.
[30] S.A Muhammed Ali, M. Anwar, A.M.Abdalla, M. Rao Somalu, A. Muchtar, $Ce_{0.80}Sm_{0.10}Ba_{0.05}Er_{0.05}O_{2-\delta}$ multi-doped ceria electrolyte for intermediate temperature solid oxide fuel cells,Ceramics Int. 43(2017)1265-1271.
[31] S. I. Ahmad, P. Koteshwar Rao, I. Ahmed Syed, Sintering temperature effect on density, structural and morphological properties of Mg- and Sr-doped ceria, J. Taibah University for Science. 10 (2016) 381–385.
[32] B. Kenney, K. Karan, Engineering of microstructure and design of a planar porous composite SOFC cathode: A numerical analysis, J. Solid State Ionics. 178 (2007) 297–306.
[33] D. Dong, J. Gao, X. Liu, G.Meng, Fabrication of tubular NiO/YSZ anode-support of solid oxide fuel cell by gel casting, J. Power Sources. 165 (2007) 217–223
[34] T. Le, Y. Yang, L. Yu, Z. Huang, F. Kang, In-situ growth of MnO_2 crystals under nanopore-constraint in carbon nanofibers and their electrochemical performance, Sci. Rep. 6 (2016) 37368.
[35] D. Neagu, G. Tsekouras, D. N. Miller, H. Menard,J. T. S. Irvine, In situ growth of nanoparticles through control of non-stoichiometry, Nature Chem. 5, 11 (2013) 916-923.
[36] A. Uhlir Jr, The Potentials of Infinite Systems of Sources and Numerical Solutions of Problems in Semiconductor Engineering, Bell Lab technical Journal. 34 (1955), 105-128.
[37] Y.-Fei Sun, Y.-Qian Zhang , B. Hua , Y. Behnamian, J. Li, S.-Hua Cui, Jian-Hui Li, J -Li Luo, Molybdenum doped $Pr_{0.5}Ba_{0.5}MnO_{3\_d}$ (Mo-PBMO) double perovskite as a potential solid oxide fuel cell anode material, J. Power Sources. 301 (2016) 237-241.
[38] W. Zhu, Z. Lu , S. Li , B. Wei, J. Miao, X. Huang, K. Chen, N. Ai, W. Su, Study on $Ba_{0.5}Sr_{0.5}Co_{0.8}Fe_{0.2}O_{3-\delta}$–$Sm_{0.5}Sr_{0.5}CoO_{3-\delta}$ composite cathode materials for IT-SOFCs, Journal of Alloys and Compounds. 465 (2008) 274–279
[39] J.T.S.Irvine, D.C.Sinclair, A.R.West. Electroceramics: characterization by impedance spectroscopy, Adv Mater. 2 (1990) 132–8.
[40] E. Barsoukov and J. R. Macdonald, Impedance Spectroscopy: Theory, Experiment, and Applications. John Wiley & Sons, Inc, 2005.
[41] S. R. Logan, The origin and status of the Arrhenius equation*J. Chem. Educ.59* ,4,(1982) 279.
[42] H. Ding, Z. Tao, S. Liu, J. Zhang, A High-Performing Sulfur-Tolerant and Redox-Stable Layered Perovskite Anode for Direct Hydrocarbon Solid Oxide Fuel Cells., Sci. Rep. 5 (2015) 18129.
[43] E. P Murray & S. A.Barnett, $(La,Sr)MnO_3$-$(Ce,Gd)O_{2-x}$ composite cathodes for solid oxide fuel cells. J. Solid State Ionics 143(2001) 265–273.
[44] M. F Liu,D.Ding,K. Blinn, X. Li, L. Nie, M. Liu, Enhanced performance of LSCF cathode through surface modification. Int. J. Hydro. Energ. 37 (2012) 8613–8620.
[45] S.B. Adler, Factors governing oxygen reduction in solid oxide fuel cell cathodes, Chem. Rev. 104 (2004) 4791–4843.
[46] R. Ku¨ngas,J. M. Vohs,R. J. Gorte, Effect of the Ionic Conductivity of the Electrolyte in Composite SOFC Cathodes, J. Electrochemical Society.158 ,6, (2011) B743-B748.

[47] S. Park, S. Choi, J. Kim, J. Shin, and G. Kim Strontium Doping Effect on High-Performance $PrBa_{1-x}Sr_xCo_2O_{5+\delta}$ as a Cathode Material for IT-SOFCs, ECS Electrochemistry Letters. 1,5, (2012) F29-F32.
[48] A. Donazzia, R. Pelosatob, G. Cordarob, D. Stucchib, C. Cristianib, G. Dotellib, I. Natali Sorac, Evaluation of Ba deficient $NdBaCo_2O_{5+d}$ oxide as cathode material for IT-SOFC, Electrochimica Acta 182 (2015) 573–587.
[49] Q.A. Huang, R. Hui, B. Wang, J. Zhang, A review of the AC impedance modeling and validation in SOFC diagnosis, Electrochem. Acta 52 (2007) 8144-8164.

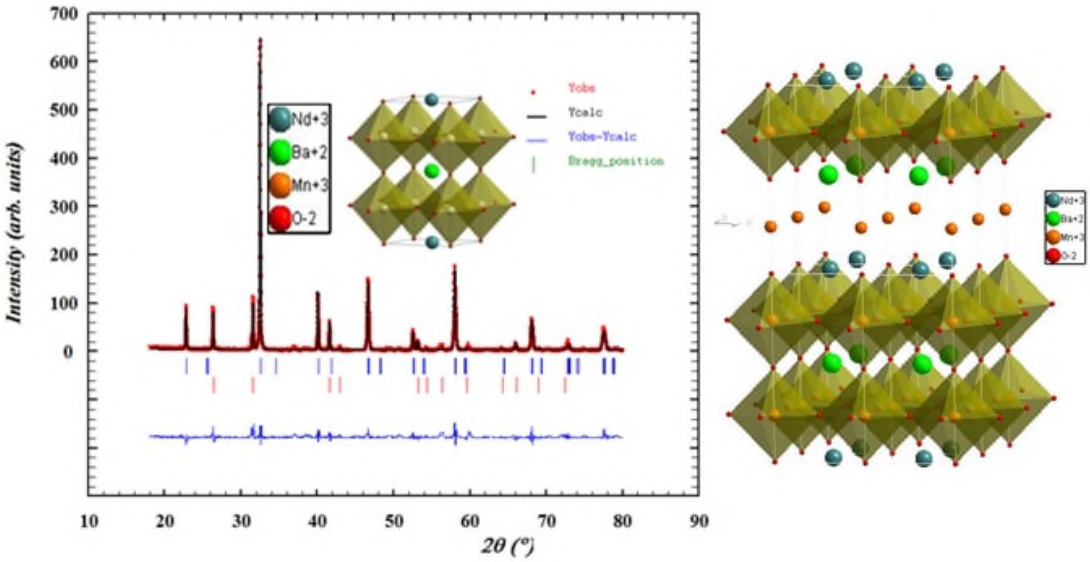

Fig.1. Rietveld refinement profileof$NdBaMn_2O_{5+\delta}$. 3D schematic diagrams is shown in the insert,in addition to the super cell structure at the right hand side.

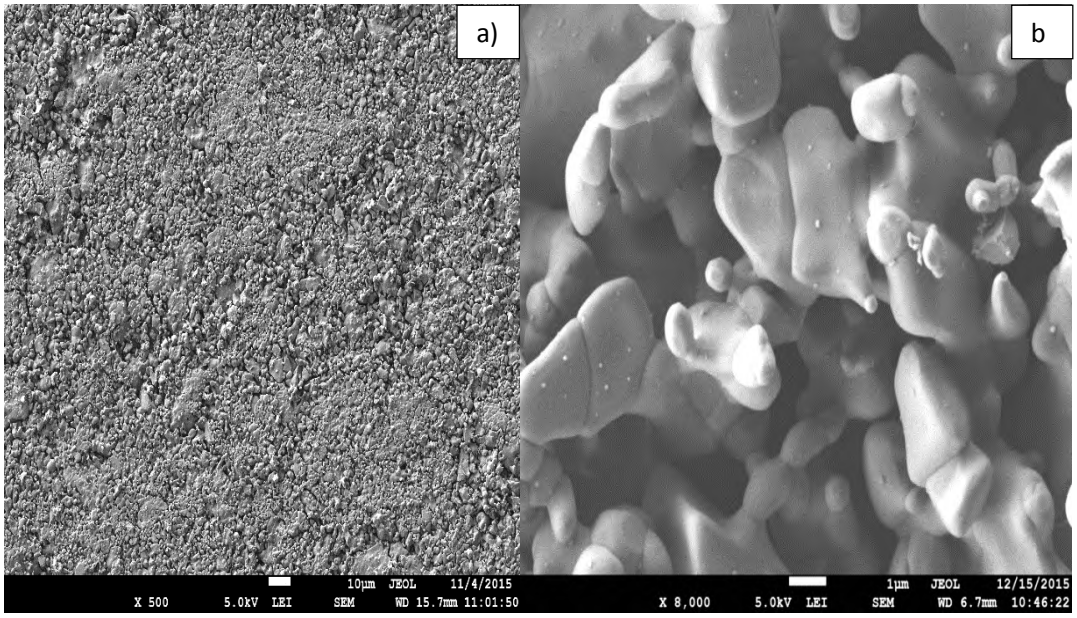

Fig. 2.SEM micrographs showing the different particle sizes and morphologies of (a) $NdBaMn_2O_5$and (b) The enlarged view of the porous structure of NBMO.

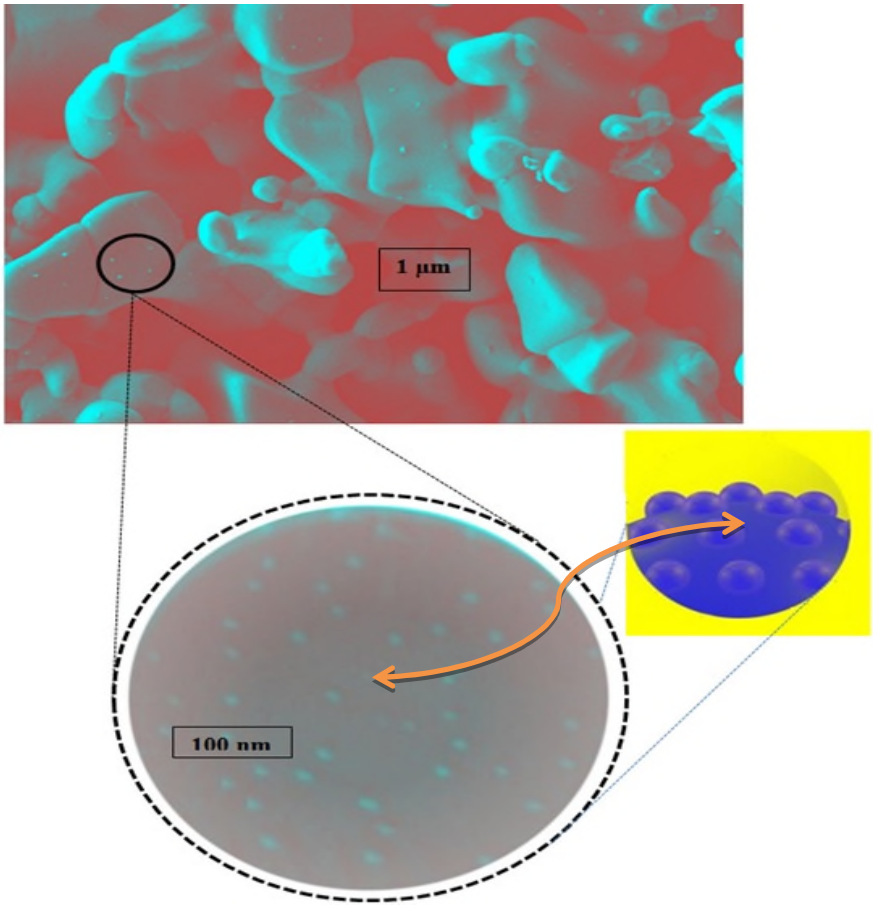

Fig. 3.SEM of the $NdBaMn_2O_{5.}$sample exhibiting nanoparticle exsolution.

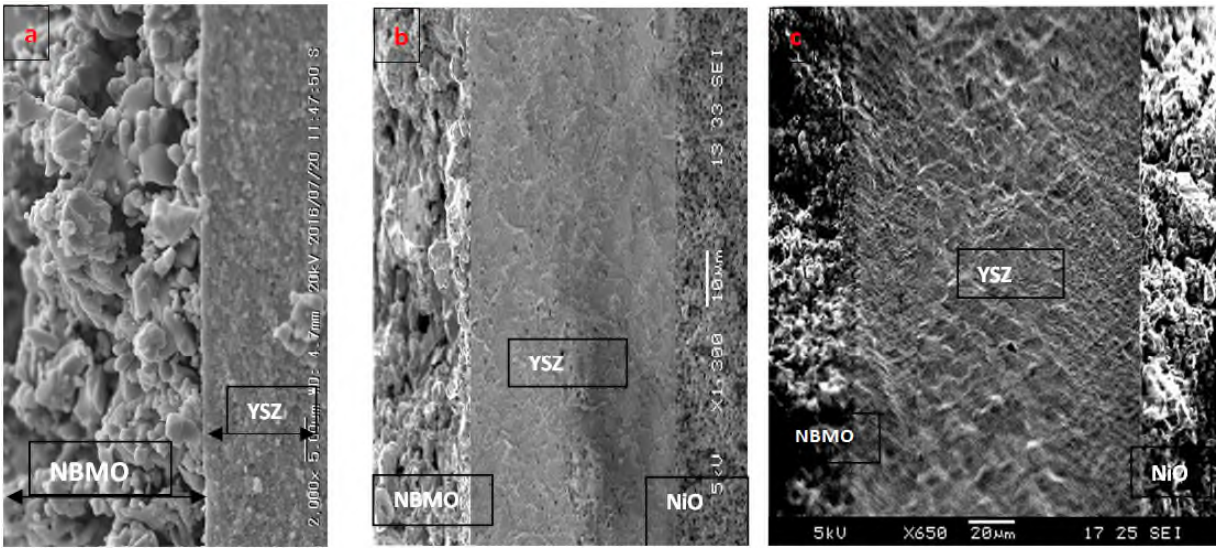

Fig. 4. Cross sectional area of a) $NdBaMn_2O_5$/YSZ/$NdBaMn_2O_5$inthe Symmetrical cell, b) before testing and c) after testing of the single cell $NdBaMn_2O_5$/YSZ/NiO-YSZ using humidified H_2 fuel.

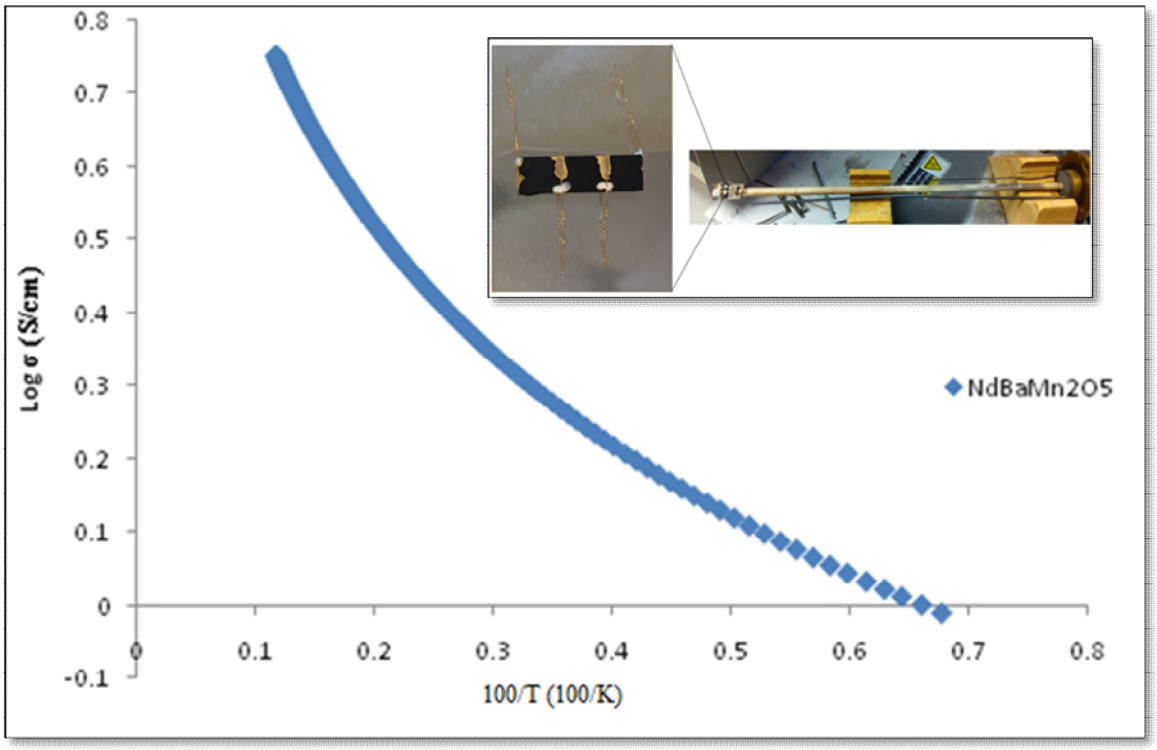

Fig. 5. Dc electrical conductivity of $NdBaMn_2O_5$ measured in air showing the highest value of 0.7 Scm^{-1} at 850 °C.

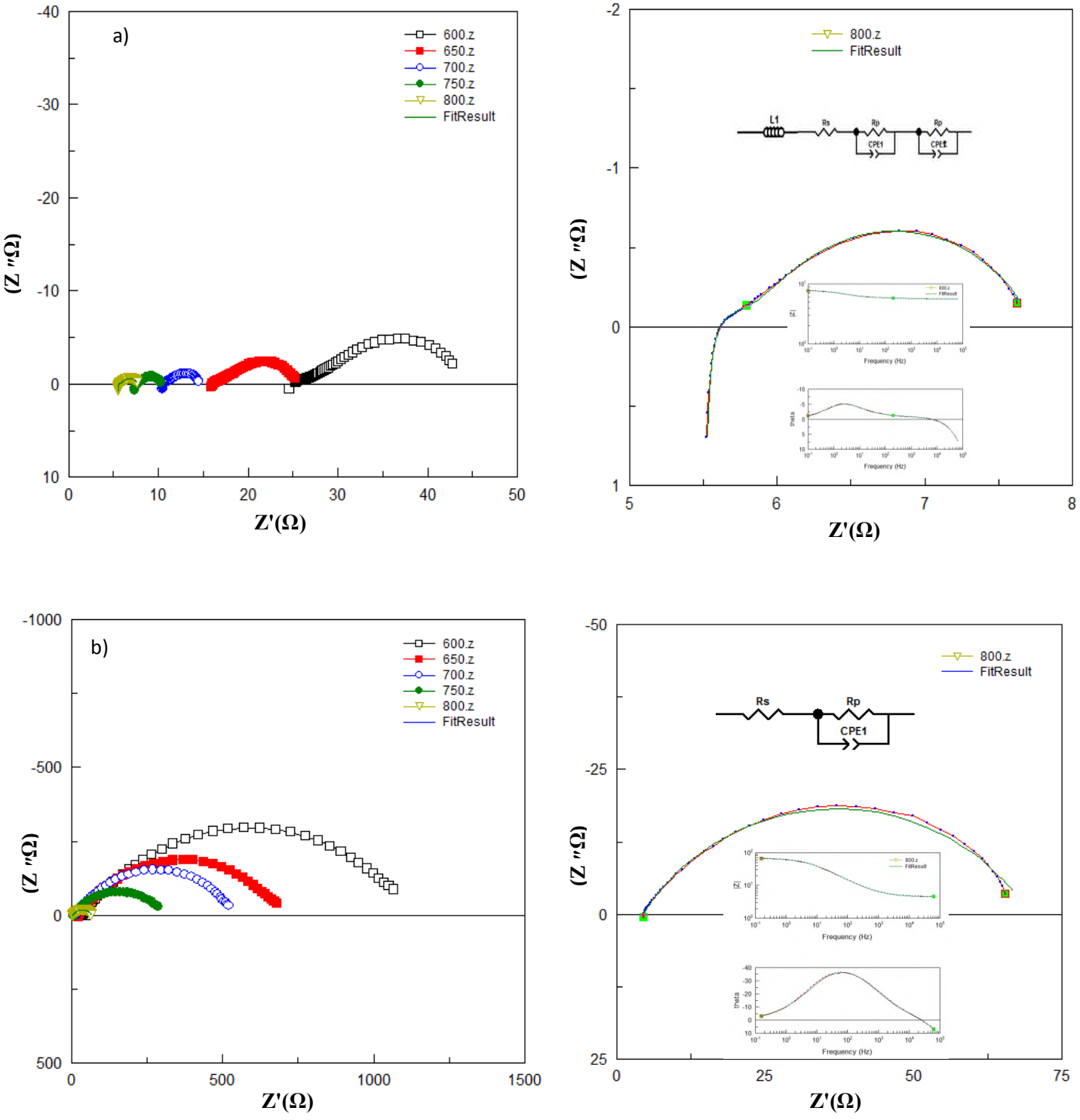

Fig. 6.EIS nyquist plots at different temperatures with fitted curve at the right hand side (equivalent circuits are shown as insert in air (a) and in 5% H_2/Ar (b).

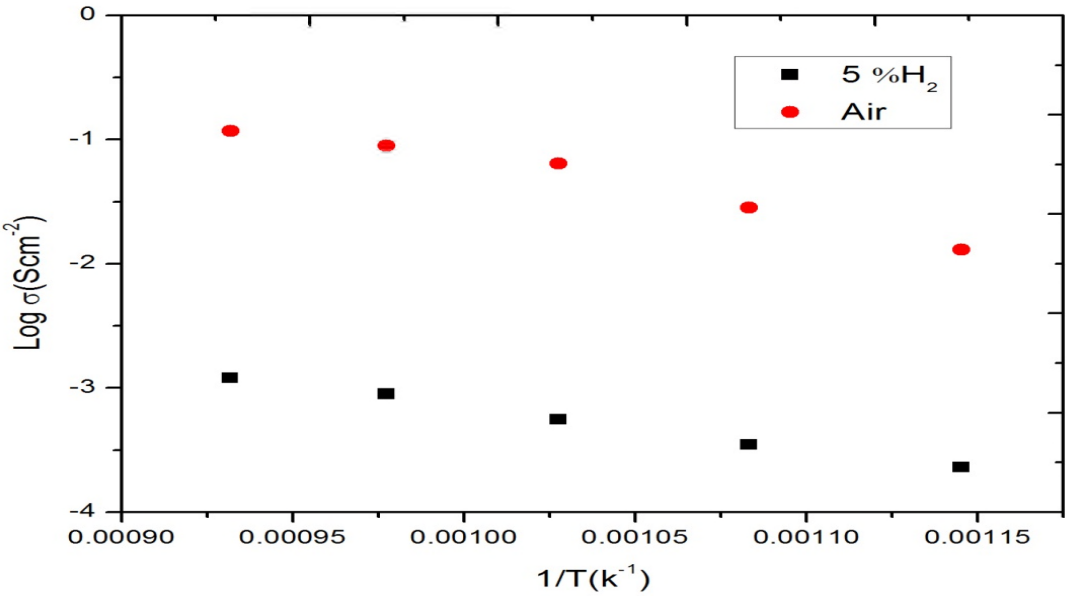

Fig. 7.$NdBaMn_2O_5$ total ionic conductivity measured in both air and 5%H_2at various temperatures from 600 °C to 800 °C.

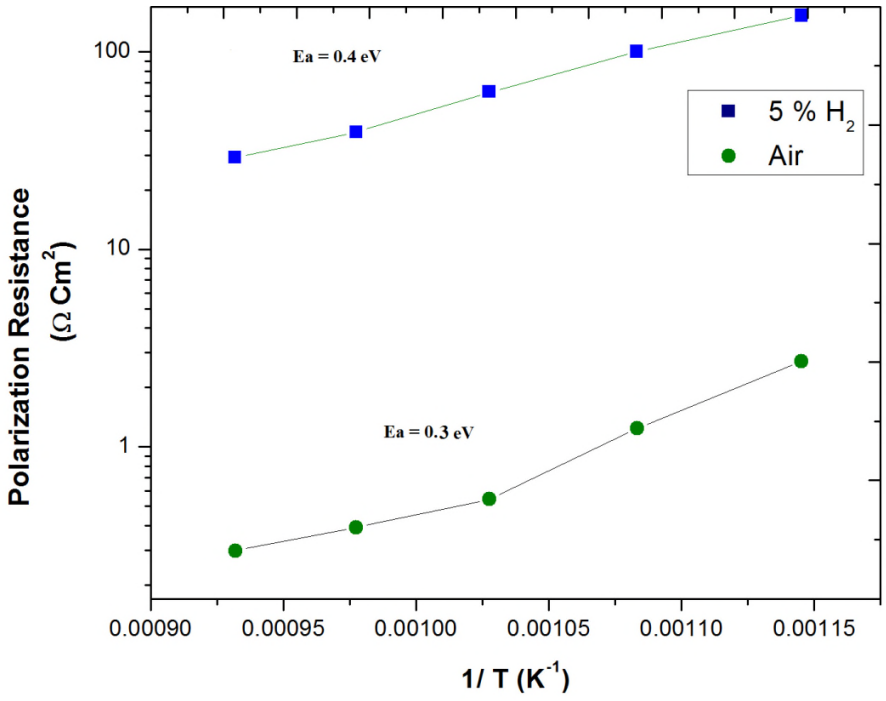

Fig. 8. Polarization resistance of NBMO measured in dry air and 5 % H_2obtained from symmetrical cell as a function of temperature with calculated activation energy.

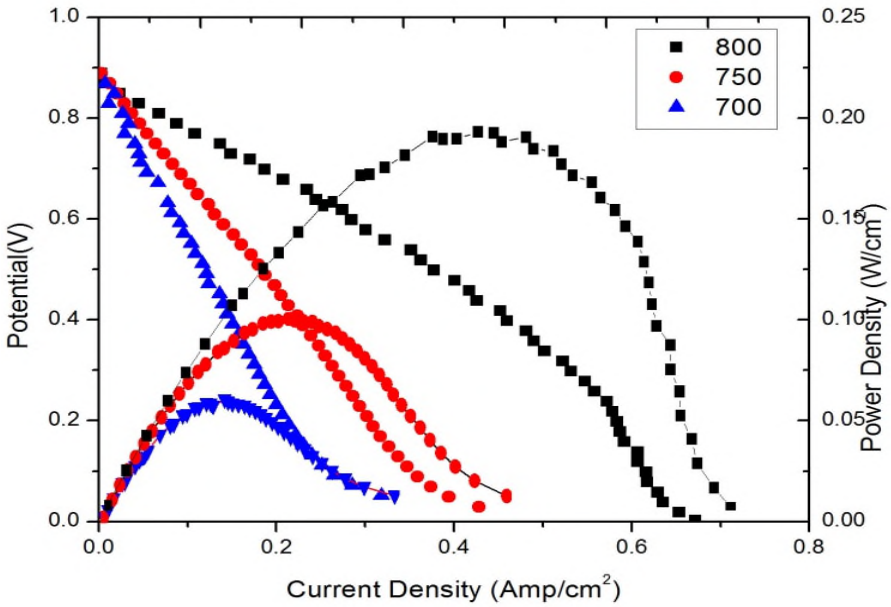

Fig. 9. Performances of the single cell Ni-YSZ/YSZ/NBMO from 700°C to 800 °C.

Table.1. Cell parameters, symmetry and space group of layered$NdBaMn_2O_{5+\delta}$ compared with some literature data.

Chemical composition	**Symmetry**	**Space group**	**a (Å)**	**b (Å)**	**c (Å)**	**V (Å^3)**
$NdBaMn_2O_5$	Orthorhombic	P*mmm*	3.8956(1)	*3.8817(6)*	7.7828(1)	117.690(2)
	Hexagonal	R-3c	5.6560(5)		4.6516(3)	148.799(2)
$NdBaMn_2O_5$*	Tetragonal	P4/*nmm*	5.6134(2)		7.7363(3)	243.773(4)
$NdBaMn_2O_5$**	Cubic	P*m3m*	3.89675(3)			59.170(9)
	Hexagonal	-	-			-

Nd$BaMn_2O_5$*ref [18]

NdBaMn_2O_5**ref [17]

Table. 2. Atomic positions and R-factors of the NBMO oxide from Rietveld refinement.

	Atomic positions			R-factors			
	x	y	z	Rp	Rwp	Rexp	χ^2
Nd	0.5	0.5	0.0	7.8	4.4	4.38	0.996
Ba	0.5	0.5	0.5				
Mn	0.0	0.0	0.7406(2)				
O1	0.0	0.5	0.2501(8)				
O2	0.5	0.0	0.2430(5)				
O3	0.0	0.0	0.5				

Table 3. The observed values of the EIS impedance by fitting of the impedance spectra in both air and 5% H_2.

T (K)	**C (F)**	**Rs (Ωcm^2)**	**R Ohmic (Ωcm^2)**	**ASR (Ωcm^2)**	***σ* *(S/cm²)***
			Air		
873	3.56E-07	24.9	42.508	1.35	1.2929E-02
923	7.23E-05	15.82	55.861	0.620	2.8240E-02
973	0.80E-03	10.42	77.591	0.272	6.4440E-02
1023	0.95E-03	7.307	177.06	0.196	8.9508E-02
1073	2.76 E-03	5.418	386.73	0.149	1.1762E-01
			5% H_2/Ar		
873	4.36- E-07	57.46	4.1748E+03	76.5	2.2896E-04
923	6.57E-05	29.47	5.6075E+03	50.2	3.4866E-04
973	5.46E-05	19.44	8.9527E+03	31.4	5.5849E-04
1023	5.55E-05	13.54	1.4341E+04	19.6	8.9166E-04
1073	5.12E-05	10.55	2.1838E+04	14.6	1.1976E-03

Table 4. Calculated theoretical values of (OCV) based on Nerst equation.

T (°C)	E_0(V)	E_T(mV)
700	1.006	1.121
750	0.997	1.078
800	0.977	1.020